Control of Inverter-Connected Sources in Autonomous Microgrids

Ian A. Hiskens   Eric M. Fleming
Department of Electrical and Computer Engineering
University of Wisconsin - Madison
Madison, WI 53706 USA

Abstract—The use of distributed generation is growing steadily, motivating a need for flexible interconnection strategies. The resulting microgrid concept allows sub-networks of sources and loads to maintain reliable operation when disconnected from the main grid. The paper presents a control strategy for inverter-based sources that supports transitioning between grid connection and autonomous operation. The controller regulates the inverter terminal voltage and the active power delivered to the AC system, and takes into account the phase-locked loop (PLL) dynamics. An example, in which two SOFC plants provide power to a microgrid, explores controller behaviour. The investigation considers disconnection from the main grid, autonomous operation, and re-synchronization with the main grid.

Keywords: Microgrid dynamics, inverter control, phase locked loops.

I. INTRODUCTION

Power systems are experiencing a rapid growth in the connection of distributed generation. A number of factor are driving this trend, including economic benefits, environmental concerns, reliability requirements, and tax incentives. Popular technologies include microturbines [1], fuel cells [2], and renewable sources such as solar and wind power [3], [4]. This list will certainly grow though, with the advent of plug hybrid electric vehicles and efficient energy storage, to mention just two technologies that are drawing significant attention.

Small generators have been dispersed throughout power systems for many years, primarily as uninterruptible power supplies. Generally these sources are not synchronized with the grid power supply though, but rather cut in when the primary supply is interrupted. Furthermore, they tend not to be interconnected with each other. Typically each source is dedicated to supplying a predefined group of loads.

With the role of distributed generation changing from backup to primary energy supply, more flexible connection strategies are required. The microgrid concept has grown out of this desire for truly interconnected operation [5], [6]. Figure 1 provides an example of a simple microgrid.[1] The generators, in this case solid oxide fuel cells (SOFCs), are grid connected. When the circuit breaker opens, however, buses 1 to 4 form an autonomous microgrid, with the two SOFC sources jointly supplying the load, while regulating voltages and frequency. Upon circuit breaker closure, the

[1]We shall explore this example further in Section IV.
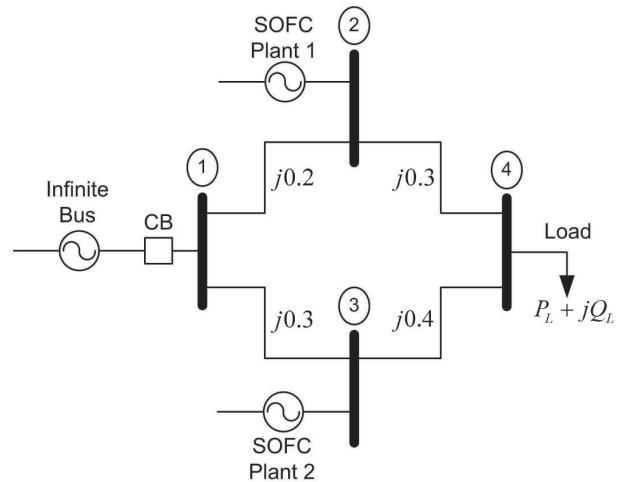

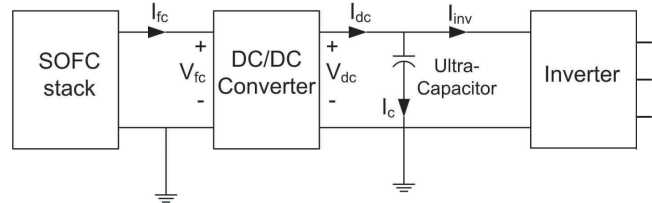Fig. 1.   Microgrid example.

Fig. 2.   DC bus topology for an SOFC source.

sources must again synchronize to the grid. A variety of approaches have been suggested for achieving this operational flexibility. An overview is provided by [7], [8], [9], [10], [11], and references therein.

Many of the newer forms of distributed generation cannot be connected directly to the AC grid. Fuel cells and solar cells, for example, effectively generate at DC. Microturbines operate at very high frequency. Grid connection therefore requires a power electronic interface. Figure 2 shows a common topology for connecting a fuel cell to the grid. The fuel cell supplies energy to the DC bus via a DC-DC converter, which acts as a current regulator. An ultra-capacitor (or perhaps a battery) maintains a fairly constant DC bus voltage by acting as an energy storage buffer, effectively isolating the fuel cell from grid demand fluctuations. A voltage-source inverter provides the connection between the DC bus and the AC grid. A control strategy for the DC current regulator is presented in [12]. This paper considers inverter controls that are required to ensure appropriate AC terminal conditions.

Fig. 3.   Inverter-grid interface.

Fig. 4.   Generic PLL block diagram.

Fig. 5.   Linearized PLL block diagram.
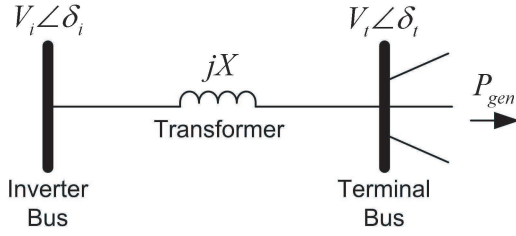
In particular, it focuses on inverters that use a phase locked loop (PLL) for synchronizing to the AC-side voltage[2].

The primary control objectives for the inverter are to deliver a specified active power to the grid, and to regulate the terminal voltage to a pre-established setpoint. However, in the event that the microgrid is operating autonomously (separated from the supporting grid), the controls must also establish the microgrid frequency. Furthermore, to be consistent with a "plug and play" connection philosophy for micro-sources, communications between sources and/or loads should be minimized. The paper presents a control strategy that allows sources to act independently, yet achieves the desired control objectives. It considers explicitly the role of the PLL, and shows that PLL dynamics can detrimentally affect controller damping. A controller design that overcomes those damping problems is proposed.

II. INVERTER MODEL

A. Inverter-grid interface model

A model for the inverter-grid interface is given in Figure 3. It consists of an "internal" bus at which the voltage-source inverter synthesizes an AC voltage waveform, and the "terminal" bus that is common with the grid. The corresponding voltage phasors are $V_i \angle \delta_i$ and $V_t \angle \delta_t$, respectively, where the phase angles are specified with respect to a global reference sinusoid of nominal frequency. These two buses are connected through a transformer, with impedance jX. All quantities are expressed in per-unit.

The inverter seeks to regulate the active power P_{gen} delivered to the grid, and the terminal bus voltage magnitude V_t. This is achieved by controlling,

1) the modulation index m of the inverter, which establishes the AC voltage magnitude V_i, and
2) the inverter firing angle, which effectively determines the phase δ_i of the synthesized voltage waveform.

It is important to keep in mind that the inverter has no knowledge of the global reference. Accordingly, the absolute phase angle δ_i is meaningless. Rather, the phase of the inverter voltage must be established relative to a local reference signal. A phase-locked loop (PLL) is often used to provide that local reference.

---

[2]Many inverters are of this form. In other cases, though, inverter firing is synchronized to an internally generated clock signal.
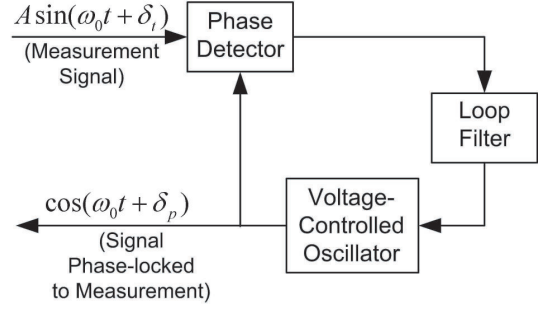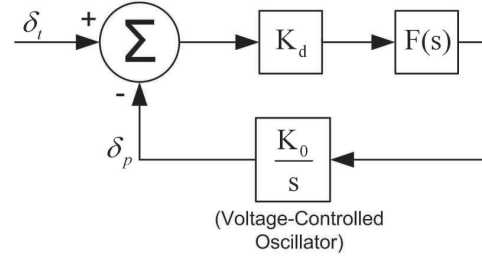
B. Phase-locked loop

Synchronizing the inverter and grid AC voltage waveforms can be achieved using a phase-locked loop (PLL). A block diagram displaying the functional components of a PLL is given in Figure 4. The measured sinusoid is mixed with the cosine generated by the PLL oscillator. This mixing process effectively establishes the phase difference between the two waveforms. That error signal is filtered and fed back to the voltage-controlled oscillator. The outcome is a signal that is phase locked to the measurement. Standard simplifying assumptions [13] allow the PLL to be modelled according to the linear block diagram of Figure 5. This model is commonly used for analysis and design of PLL-based systems [13]. Note though that the PLL has no knowledge of the global synchronous reference, and hence cannot determine the absolute angles δ_t and δ_p. The phase difference $\delta_t - \delta_p$ is, however, available locally.

Relating back to the inverter-grid connection of Figure 3, the PLL input is given by the terminal bus voltage $v_t(t)$, which has phase angle δ_t relative to the global reference sinusoid. If the grid frequency experiences a constant offset from nominal, then δ_t will by time-varying. To achieve zero offset between δ_t and δ_p under such circumstances, the PLL transfer function $F(s)$ should take the form

$$F(s) = \frac{K}{s}.$$

From Figure 5, this gives $\delta_p = \frac{K_d K K_o}{s^2}(\delta_t - \delta_p)$. Rewriting as a differential equation, with $K_3 = K_d K K_o$, and defining

$$\dot{\delta}_p = \omega_p \tag{1}$$

gives

$$\dot{\omega}_p = K_3(\delta_t - \delta_p). \tag{2}$$

587

An estimate of the deviation of system frequency from nominal is provided by ω_p.

III. INVERTER CONTROL

As mentioned previously, the control objectives are to regulate the terminal bus voltage magnitude V_t, and the active power delivered to the grid P_{gen}. The first objective can be achieved by simple integral control

$$\dot{m} = K_1(V_{set} - V_t) \tag{3}$$

where V_{set} may be constant, or may follow a droop characteristic that is dependent upon the reactive power delivered to the grid. The inverter internal bus voltage is then given by

$$V_i = \frac{mV_{dc}}{V_{base}} \tag{4}$$

where V_{base} is the per-unit base voltage for the DC bus and inverter.

From Figure 3, the active power delivered to the grid is given by

$$P_{gen} = \frac{V_i V_t}{X} \sin(\delta_i - \delta_t). \tag{5}$$

This quantity must also be equal to the power on the DC side of the inverter after making the per-unit conversion,

$$P_{gen} = \frac{V_{dc} I_{inv}}{P_{base}}. \tag{6}$$

Assuming V_i and V_t remain relatively constant, regulation of P_{gen} can be achieved by controlling the angle difference $\delta_i - \delta_t$. The PLL output δ_p provides a filtered version of δ_t though, so it is preferable to control

$$\theta = \delta_i - \delta_p. \tag{7}$$

Integral control gives,

$$\dot{\theta} = K_2(P_{set} - P_{gen}). \tag{8}$$

The active power setpoint P_{set} is usually dependent upon a droop characteristic of the form

$$P_{set} = P^0 - R\omega_p, \tag{9}$$

where ω_p is the estimated frequency deviation provided by the PLL, see (1), and R is the droop constant. The following analysis shows, however, that interactions between this P_{gen} controller and the PLL dynamics cause sustained oscillations.

Rearranging (7) and substituting into (2) gives

$$\dot{\omega}_p = K_3(\delta_t - \delta_i + \theta). \tag{10}$$

Referring to (5), if P_{gen}, V_i and V_t are constant, then $\delta_i - \delta_t$ must also be constant. Under those conditions, differentiating (10) and substituting (8) and (9) gives

$$\ddot{\omega}_p = K_3 \dot{\theta}$$
$$= K_2 K_3(P^0 - R\omega_p - P_{gen})$$

which implies

$$\ddot{\omega}_p + K_2 K_3 R\omega_p = K_2 K_3(P^0 - P_{gen}). \tag{11}$$

This second order system is undamped. Any disturbance will lead to unattenuated oscillations in ω_p, even when P_{gen}, V_i and V_t are all constant.

Viable control requires the addition of a damping term to (11). This can be achieved by adding an extra term into (2),

$$\dot{\omega}_p = K_3(\delta_t - \delta_p) + K_4 \dot{\theta}. \tag{12}$$

Differentiating, as above, and making similar substitutions results in

$$\ddot{\omega}_p = K_3 \dot{\theta} + K_4 \ddot{\theta}$$
$$= K_2 K_3(P^0 - R\omega_p - P_{gen}) + K_2 K_4(-R\dot{\omega}_p)$$

and hence

$$\ddot{\omega}_p + K_2 K_4 R\dot{\omega}_p + K_2 K_3 R\omega_p = K_2 K_3(P^0 - P_{gen}). \tag{13}$$

Further rearranging gives

$$\frac{1}{K_2}\ddot{\omega}_p + K_4 R\dot{\omega}_p + K_3 R\omega_p = K_3(P^0 - P_{gen}) \tag{14}$$

which reveals that $1/K_2$ acts like an inertia constant, and damping is provided by $K_4 R$.

Defining the algebraic relationship

$$x = \omega_p - K_4\theta \tag{15}$$

allows (12) to be rewritten

$$\dot{x} = K_3(\delta_t - \delta_p). \tag{16}$$

Bringing the complete control strategy together gives,

$$\dot{m} = K_1(V_{set} - V_t)$$
$$\dot{\theta} = K_2(P_{set} - P_{gen})$$
$$\dot{x} = K_3(\delta_t - \delta_p)$$
$$\dot{\delta}_p = \omega_p$$
$$0 = V_i - \frac{mV_{dc}}{V_{base}}$$
$$0 = P_{set} - (P^0 - R\omega_p)$$
$$0 = \theta - (\delta_i - \delta_p)$$
$$0 = x - (\omega_p - K_4\theta)$$
$$0 = P_{gen} - \frac{V_{dc} I_{inv}}{P_{base}}.$$

The PLL and power regulator are described by the block diagram of Figure 6.

IV. MICROGRID EXAMPLE

The microgrid shown in Figure 1 will be used to illustrate the dynamic behaviour of the model components. SOFC plants are located at buses 2 and 3, and a constant power load is connected to bus 4. Bus 1 forms the interface between the microgrid and the rest of the power system, which is modelled as an infinite bus.

All of the AC quantities are expressed as per-unit values. A power base of 100 kVA is used in connecting the SOFC plant models to the inverter and grid models. A voltage base of 240 V was chosen for the DC buses and inverters. Since the DC bus setpoint voltage is 480 V, this causes the nominal
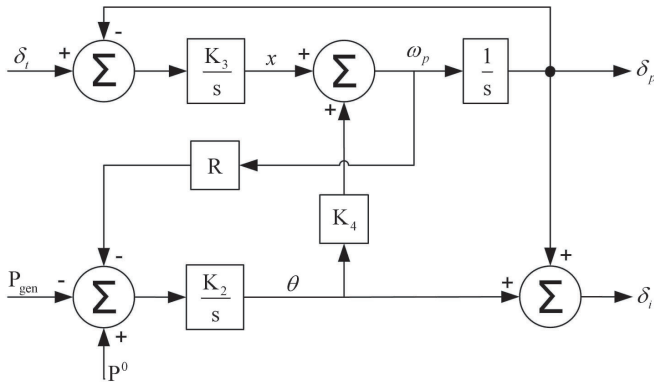
Fig. 6. PLL and active power regulation block diagram.

Fig. 7. Power output of the inverters.

Fig. 8. PLL frequency deviation of inverters.

value of the modulation index to be 0.5. The actual voltage of the grid is irrelevant.

For this example, both inverters have the parameters given in Table I. Plant 1 has a power setpoint of 0.7 pu (70 kW), and Plant 2 has a power setpoint of 0.6 pu (60 kW). The active and reactive power of the load, P_L and Q_L, are 1.7 pu and 0.6 pu, respectively, and the voltage of the infinite bus is set to 1 pu. The circuit breaker (CB) connecting bus 1 to the rest of the grid is initially closed. The two fuel cell plants together supply 1.3 pu of the active power demanded by the load. The remaining 0.4 pu active power is drawn from the main grid through bus 1. At 1 s, the CB opens. The constant load must now be supplied by the fuel cell plants. At 7 s, the CB is signaled to close, but closing is prevented until the voltage magnitude appearing across the CB contacts reduces to a given threshold. For this simulation, the threshold is set to $\sqrt{0.05}$ pu.[3] Consequently, the CB actually closes at 13.01 s.

TABLE I
SOFC-INVERTER PLANT PARAMETERS.

parameter	value
K_1	10
K_2	20
K_3	20
K_4	10
R	0.4
X	0.2pu
V_{set}	1pu
V_{dc}^{set}	480V

Figure 7 shows the power delivered by each of the inverters over the simulation period, and Figure 8 shows the frequency deviation given by the inverter PLLs. When the microgrid is initially disconnected from the main grid, the power supplied from the DC bus immediately increases to compensate for the lost grid supply. Microgrid frequency drops in accordance with the droop characteristic. Note that Plant 1, which has a higher power setpoint, overshoots when the CB opens, while Plant 2 does not. The sum of the two power outputs must always equal the active power of the

[3]For numerical reasons, the simulation actually monitors the square of the voltage magnitude.
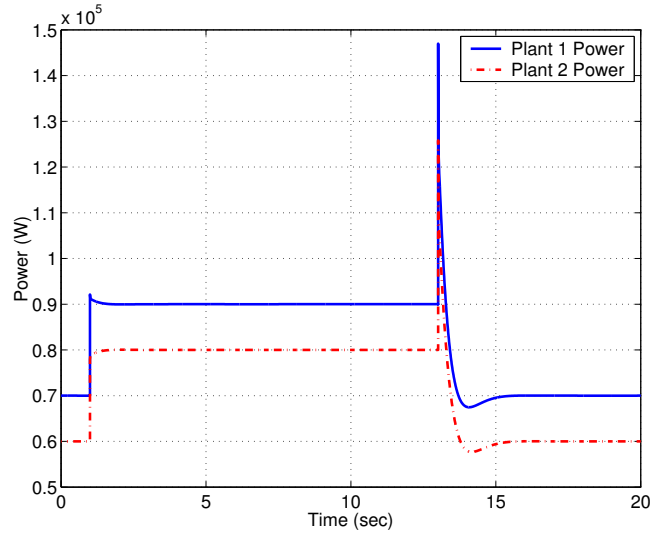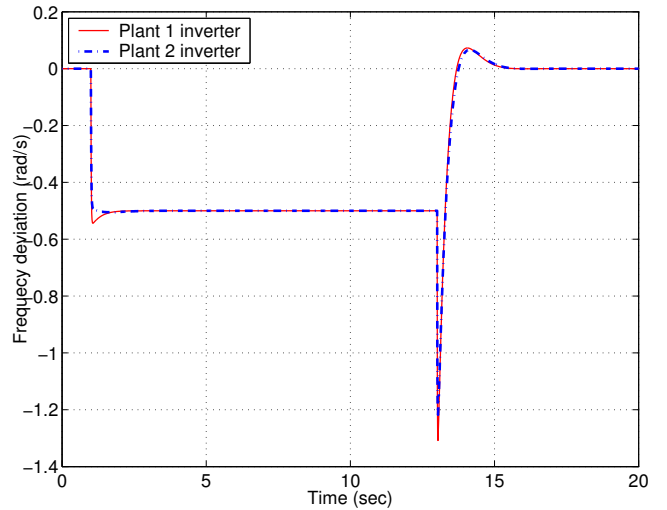
load while the CB is open.

When the CB recloses, the phase relationship between the inverter voltages (which cannot change instantaneously) and the grid is such that active power initially flows from the microgrid to the infinite bus. Therefore, both plants see a power spike immediately following the reconnection. The inverter controls respond accordingly, with active power outputs quickly returned to their pre-disturbance values, and microgrid frequency restored to the nominal value.

Note that the grid model uses a phasor representation for voltages and currents, and therefore does not provide an accurate representation of fast transient behaviour [14]. In reality, the transformer inductance would limit the rate of change of the inverter current, so the spike would be smaller than indicated in Figure 7.

Figure 9 shows angle behaviour during the disturbance. (Only Plant 1 inverter quantities are shown.) When the CB opens, the inverter terminal bus voltage undergoes an imme-
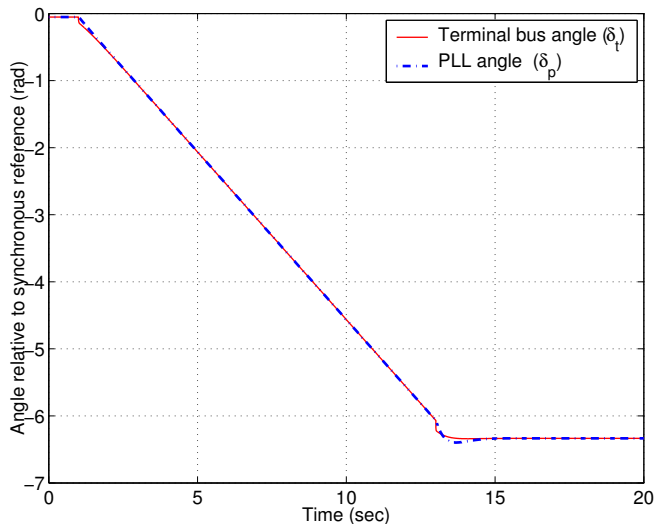
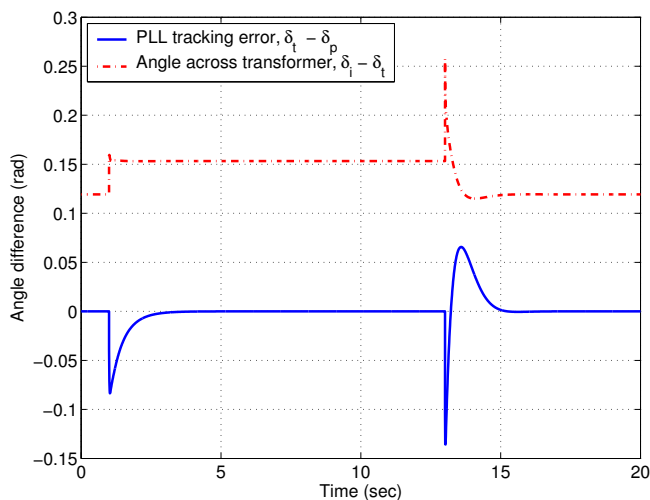Fig. 9. Plant 1 inverter angle behaviour relative to a global reference.

Fig. 10. Plant 1 inverter angle differences.

diate phase shift. Over the subsequent period of autonomous operation, the microgrid frequency is below nominal. Accordingly, the microgrid phase angle, relative to a global reference at nominal frequency, displays a steady decrease. This continues until the CB recloses. At that instant, the microgrid voltages are out of phase with the stronger system. In response, the inverter terminal bus phase angle adjusts very rapidly, quickly settling to a value that lags its initial value by exactly 2π radians.

Figure 9 also shows that the PLL angle closely tracks the terminal bus angle. The difference between these quantities is shown more clearly in Figure 10. It can be seen that the controller is effective in rapidly driving this difference to zero. The angle difference across the inverter transformer is also shown in Figure 10. Notice that when the CB closes, the resulting phase shift in the inverter terminal bus voltage causes a spike in the angle difference across the inverter transformer. That spike in angle difference underlies the spike in active power P_{gen} observed in Figure 7.

V. CONCLUSIONS

Many distributed generation sources, such as fuel cells and solar cells, cannot be connected directly to AC systems. A power electronic interface is required, with a common topology consisting of a DC-AC voltage-source inverter. The proposed inverter control strategy allows autonomous microgrids to be supplied solely by such inverter-based sources.

The inverter controls regulate the power delivered to the grid, the terminal voltage, and also maintain the microgrid frequency. It has been shown that interactions between inverter controls and PLL dynamics can potentially give rise to sustained oscillations. However, by incorporating the PLL behaviour into the controller design, these oscillations can be eliminated.

An example system, in which two SOFC plants provide power to a microgrid, has been presented. In the example, the microgrid was initially connected to the main grid, and was subsequently disconnected. During autonomous operation, the microgrid operated at a frequency below nominal due to droop control. At reconnection, microgrid voltages were out of phase with the stronger system. This resulted in a step change in the phase angle across each inverter transformer, causing a spike in their power outputs. Inverter controls quickly responded, returning the power outputs to their setpoint values, and the microgrid frequency to nominal.

REFERENCES

[1] R. Staunton and B. Ozpineci, "Microturbine power conversion technology review," Oak Ridge National Laboratory Report ORNL/TM-2003/74, April 2003.
[2] J. Larminie and A. Dicks, *Fuel Cell Systems Explained*, 2nd ed. Chinchester, England, UK: John Wiley and Sons, 2003.
[3] G. Boyle (Editor), *Renewable Energy: Power for a Sustainable Future*, 2nd ed. Oxford, UK: Oxford University Press, 2004.
[4] T. Ackermann (Editor), *Wind Power in Power Systems*. England: John Wiley and Sons, 2005.
[5] R. Lasseter, A. Akhil, C. Marnay, J. Stephens, J. Dagle, R. Guttromson, S. Meliopoulos, R. Yinger, and J. Eto, "Integration of distributed energy resources: The CERTS microgrid concept," Lawrence Berkeley National Laboratory Report LBNL-50829, April 2002.
[6] N. Hatziargyiou, H. Asano, R. Iravani, and C. Marnay, "Microgrids," *IEEE Power and Energy Magazine*, vol. 5, no. 4, pp. 78–94, July/August 2007.
[7] K. De Brabandere, B. Bolsens, J. Van den Keybus, A. Woyte, J. Driesen, and R. Belmans, "A voltage and frequency droop control method for parallel inverters," *IEEE Transactions on Power Electronics*, vol. 22, no. 4, pp. 1107–1115, July 2007.
[8] T. Green and M. Prodanović, "Control of inverter-based micro-grids," *Electic Power Systems Research*, vol. 77, pp. 1204–1213, 2007.
[9] J. Guerrero, J. Matas, L. García de Vicuña, M. Castilla, and J. Miret, "Wireless-control strategy for parallel operation of distributed-generation inverters," *IEEE Transactions on Industrial Electronics*, vol. 53, no. 5, pp. 1461–1470, October 2006.
[10] J. Peças Lopes, C. Moreira, and A. Madureira, "Defining control strategies for microgrids islanded operation," *IEEE Transactions on Power Systems*, vol. 21, no. 2, pp. 916–924, May 2006.
[11] P. Piagi, "Microgrid control," PhD Thesis, Department of Electrical and Computer Engineering, University of Wisconsin-Madison, 2005.
[12] E. Fleming and I. Hiskens, "Dynamics of a microgrid supplied by solid oxide fuel cells," in *Proceedings of the Symposium on Bulk Power System Dynamics and Control - VII*, Charleston, SC, August 2007.
[13] D. Abramovitch, "Phase-locked loops: a control centric tutorial," in *Proceedings of the American Control Conference*, Anchorage, AK, May 2002.
[14] P. Sauer, B. Lesieutre, and M. Pai, "Transient algebraic circuits for power system dynamic modeling," *International Journal of Electrical Power and Energy Systems*, vol. 15, no. 5, pp. 315–321, 1993.